



Photochemical &
Photobiological
Sciences

Role of Constitutive Nitric Oxide Synthases in Dynamic Regulation of Autophagy Response of Keratinocytes Upon UVB Exposure

Journal:	<i>Photochemical & Photobiological Sciences</i>
Manuscript ID	PP-ART-08-2020-000280
Article Type:	Paper
Date Submitted by the Author:	19-Aug-2020
Complete List of Authors:	Bahamondes Lorca, Veronica; Ohio University, Chemistry & Biochemistry Wu, Shiyong; Ohio University, EBI;

SCHOLARONE™
Manuscripts

Role of Constitutive Nitric Oxide Synthases in Dynamic Regulation of Autophagy Response of Keratinocytes Upon UVB Exposure

Verónica A. Bahamondes Lorca^{a, b} and Shiyong Wu^{a*}

^a *Edison Biotechnology Institute and Department of Chemistry and Biochemistry, Ohio University, Athens, Ohio 45701*

^b *Departamento de Tecnología Médica, Facultad de Medicina, Universidad de Chile, Santiago, Chile*

* To whom all correspondence should be addressed: Edison Biotechnology Institute. Ohio University. Building 25, The Ridges. Athens, OH 45701. Phone: 740-597-1318. Fax: 740-593-4795. Email: wus1@ohio.edu.

Emails

Verónica A. Bahamondes Lorca: vb699614@ohio.edu

Shiyong Wu: wus1@ohio.edu

ORCID

Verónica A. Bahamondes Lorca: 0000-0002-0488-2472

Shiyong Wu: 0000-0002-4104-4160

Role of Constitutive Nitric Oxide Synthases in Dynamic Regulation of Autophagy Response of Keratinocytes Upon UVB Exposure

Abstract: Ultraviolet B (UVB) radiation induces autophagy responses, which play a role in the regulation of oncogenic processes of the irradiated cells. However, the mechanism of autophagy responses post-UVB remains to be fully elucidated. Previous studies indicate that UVB induces the activation and uncoupling of constitutive nitric oxide synthases (cNOS), which produce nitric oxide and peroxynitrite, both have been shown to regulate autophagy responses. In this study, the UVB-induced autophagy responses were analysed in cell line- and UVB dose-dependent manners, and the role of cNOS in UVB-induced autophagy responses was also studied. Our data showed that UVB induces both autophagosome formation and degradation, and that cNOS is involved in the regulation of autophagy responses post-UVB. Both nitric oxide and peroxynitrite, the two products that are produced in cells immediately after UVB exposure, could upregulate autophagy in a dose-dependent manner. Furthermore, cNOS is involved in the UVB-induced downregulation of SQSTM1/p62, a scaffold protein used as a reporter of autophagy response. However, the cNOS-mediated reduction of SQSTM1/p62 is autophagy-independent post-UVB. Our results indicated that autophagy responses post-UVB are a dynamic balance of autophagosome formation and degradation, with cNOS playing a role in regulation of the balance.

Keywords: Autophagic flux; constitutive Nitric Oxide Synthases (cNOSs); keratinocytes; nitric oxide; peroxynitrite; ultraviolet radiation B.

Abbreviations: cNOS: constitutive Nitric Oxide Synthase; CQ: Chloroquine; HEKa: Human Epidermal Keratinocytes; MAP1LC3A/B: Microtubule-associated proteins 1A/1B light chain 3 alpha/beta; L-NAME: N_ω-Nitro-L-arginine methyl ester hydrochloride; MEF: murine embryonic fibroblast; NO[•]: nitric oxide; O₂^{• -}: superoxide radical; ONOO⁻: peroxynitrite; SIN-1: 3-Morpholino-sydnonimine; SQSTM1/p62: sequestosome-1; SNAP: S-Nitroso-N-acetyl-DL-penicillamine; UVB: Ultraviolet B.

Introduction

After ultraviolet B (UVB) radiation, a rapid increase in the nitric oxide (NO[•]) and superoxide radical (O₂^{•-}) levels has been described in epithelial cells (1-4). Previously, we reported that NO[•] and O₂^{•-} levels in keratinocytes are elevated in the early phase after UVB (0-6 h) due to the activation and uncoupling of constitutive nitric oxide synthase (cNOS) respectively (2, 4). The O₂^{•-} could quickly react with NO[•] to form peroxynitrite (ONOO⁻), leading to a lower [NO[•]]/[ONOO⁻] ratio in the UVB irradiated keratinocytes (4). Oxidative stress, through reactive oxygen and nitrogen species such as hydrogen peroxide (H₂O₂), NO[•], and ONOO⁻, regulates cellular responses. One of these responses is the macro-autophagy (generally just referred as autophagy) mechanism (5-10).

Autophagy is regulated by different stress stimuli (e.g. nutrient starvation and oxidative stress) having a constitutive and an adaptive role in cells. For example, autophagy eliminates damaged or senescent cellular components (constitutive autophagy), and provides energy in case of metabolism alteration and nutrient starvation, through the degradation and reutilization of building blocks such as amino acids, nucleotides, and fatty acids (adaptive autophagy) (11). Autophagy participates in the degradation of aggregated proteins, organelles, etc. by lysosomes, through the formation of autophagosomes and its fusion with lysosomes (11). In the skin, autophagy has been described to be important in keratinocytes for cell differentiation (12-14), melanosome degradation (14, 15), immune response-inflammation (14, 16, 17), aging-senescence (14, 18-20), and protection against stress (14, 20-22). Nevertheless, after UVB exposure, the autophagy response in keratinocytes is still not very well understood; and indeed, reports about the autophagy response are contradictory (21, 23).

Previously, our group has characterized the early imbalance between NO[•] and ONOO⁻ after UVB treatment due to cNOS activation and its uncoupling (2, 4). In addition, we observed that cNOS activation after UVB regulates the phosphorylation of eukaryotic translation initiation factor 2 subunit alpha (eIF2 α) (24), the activation of nuclear factor kappa-light-chain-enhancer of activated B cells (NF- κ B), and the expression of I κ B kinase (IKK) in the early phase (6 h) after UVB irradiation (25); being all of them related with the regulation of autophagy (26-32). In this study, we further analysed the autophagy responses

in various cell lines in a UVB dose- and time-dependent manner and determined the role of cNOS in autophagy responses post-UVB.

Materials and Methods

Cell culture. Human Epidermal Keratinocytes, adult (HEKa) cells (Gibco™, C-005-5C) and Human Epidermal Keratinocytes, neonatal (HEKn) cells (Gibco™, C-0015C) (passage 3 to 6) were grown in EpiLife medium (Gibco™, M-EPI-500-CA) supplemented with Human Keratinocyte Growth Supplement (Gibco™, S-001-5), at 37°C with 5 % CO₂. Human keratinocytes HaCaT cells at passage 5 to 11 (AddexBio, T0020001) and mouse embryonic fibroblast (MEF) cells were grown in Dulbecco's minimal essential medium (Corning™, Cellgro™, 10-013-CV) supplemented with 10 % v/v fetal bovine serum and 1 % v/v penicillin/streptomycin, at 37°C with 5 % CO₂.

UVB irradiation. UVB was generated from a bench XX-15 series UV lamp (UVP Inc.) equipped with a 15 Watts tube (302 nm, UVP Inc.) The intensity of UVB was calibrated using a UVP model UVX digital radiometer (UVP Inc.) after lamp warmed up for at least 5 min. 10, 25 and 50 mJ/cm² of UVB were used with a dose rate of 0.85 milliwatts/cm² per second. Prior to UVB radiation, the medium with or without drugs was removed to then be added back after radiation.

Drug treatments. S-Nitroso-N-acetyl-DL-penicillamine (SNAP, Cayman Chemical, 82250) was prepared on Dimethyl sulfoxide (DMSO, Millipore Sigma, D2438) and diluted prior to use in cell medium to final concentrations of 0.0125, 0.05 and 0.1 mM. 3-Morpholino-sydnonimine (SIN-1, Cayman Chemical, 82220) was prepared in DMSO and diluted prior to use in cell medium to final concentrations of 0.0015, 0.005, 0.015 and 0.03 mM. SNAP and SIN-1 were kept in the medium during 3 h until protein extraction. Chloroquine (CQ, Sigma-Aldrich®, C6628) was diluted in cell medium to a final concentration of 50 µM and was added 1 h before UVB or NO•/ONOO⁻ donor treatment and kept for the whole period until protein analysis. N_ω-Nitro-L-arginine methyl ester hydrochloride (L-NAME, Sigma-Aldrich®, N5751) was prepared prior to use in cell medium to a final concentration of 1 mM. L-NAME was added to the cells 1 h before UVB

and continuously kept after irradiation until protein extraction.

Western blot analysis. Radioimmunoprecipitation assay (RIPA) buffer (100 mM Tris-HCl, 2% v/v Triton X-100, 300 mM NaCl, 0.2% w/v SDS, 10 mM EDTA, and 1% w/v Sodium deoxycholate) with the proteinase inhibitor mixture (Complete™, Mini, EDTA-free Protease Inhibitor Cocktail, Roche, 11836170001) was used to lyse the cells. Cells were scraped directly from the plates, pipetted and incubated on ice during 30 min vortexing them each 5 min. The lysate was centrifuged at 12,000 rpm at 4°C for 10 min and the supernatant was saved. Protein concentration was measured using the DC protein assay (Bio-Rad Laboratories, Inc) according to manufacturer instructions. Proteins were separated by SDS-PAGE and transferred to PVDF membrane (pore size 0.45 µm, Immobilon-P, Millipore, IPVH00010). The membrane was blocked in 5 % w/v milk in Tris-buffered saline plus Tween 20 (TBST) for 1 h and then incubated overnight with the antibodies anti LC3A/B-I and II (1:1000, Cell Signaling Technology®, 4108), β-actin (1:1500, Santa Cruz Biotechnology, sc-47778), SQSTM1/p62 (1:1000, Santa Cruz Biotechnology, sc-28359) diluted on TBST. After washing, the membranes were incubated with the corresponding HRP-conjugated-secondary antibody for 1 h at room temperature (Cell Signaling Technology®) in 5 % w/v milk in TBST. The membranes were developed using the West Pico Super Signal chemiluminescent substrate (Thermo Fisher Scientific, 34580) or the Western Sure PREMIUM Chemiluminescent Substrate (LI-COR Biosciences, 926-95000). Images were obtained from Odyssey® Fc Imaging System (LI-COR Biosciences) and quantified using the software Image Studio Lite (LI-COR Biosciences).

Autophagy and Autophagy flux evaluation. The most valid system described to study autophagy is to determine the “autophagy flux”, which involves the dynamic process of autophagosome synthesis, delivery of autophagic substrates to the lysosome, and degradation of autophagic substrates inside the lysosome (33, 34). MAP1LC3A/B-II levels were identified though immunoblot using an antibody that recognize MAP1LC3A/B (Cell Signaling Technology®, 4108). To inhibit autophagosomes degradation and recycling of MAP1LC3A/B-II, cells were treated with CQ 50 µM (Sigma-Aldrich®, C6628) 1 h before and continuously after UVB irradiation until protein extraction.

Immunofluorescence staining of MAP1LC3A/B and SQSTM1/p62. Cells were fixed and permeabilized with cold methanol for 10 min. After washing them with PBS, cells were blocked with 5% w/v BSA for 1 h at room temperature. Cells were incubated with the primary antibodies against MAP1LC3A/B (1:100, Cell Signaling Technology®, 4108) and SQSTM1/p62 (1:100, Santa Cruz Biotechnology, sc-28359) overnight at 4°C. After washing with PBS, cells were incubated with the corresponding secondary antibodies (1:200, Vector laboratories) plus DAPI (4'-6-diamidin-2'-phenylindol-dihydrochlorid) for 1 h at room temperature. Pictures were taken using a confocal microscope (Zeiss).

Statistical analysis. Each experiment was repeated at least three times. For blots quantification and comparison of samples under different conditions; samples were separated electrophoretically in the same gel, and in its defect, they were transferred together to the same membrane. The bar plots are expressed as the mean values \pm S.D. The significance of the differences between mean values was assessed using Student's t-test. p-values smaller than 0.05 were considered significant.

Results

UVB induces both autophagosome synthesis and degradation.

To analyse autophagosome synthesis and degradation, MAP1LC3A/B-II protein levels were evaluated at 3 h post-UVB in the presence or absence of chloroquine (CQ), which impairs the fusion autophagosome-lysosome and sequentially inhibits autophagosome degradation and recycling of MAP1LC3A/B-II (33-35). Our data shows that the level of MAP1LC3A/B-II was not altered in HaCaT cells at 3 h after UVB exposure alone (Fig. 1A, Lanes 1-4). However, in the presence of CQ, the level of MAP1LC3A/B-II was increased by approximately 20% in the cells after UVB (25 mJ/cm²) exposure (Fig. 1A, Lane 7 vs. 5), and slightly increased non-statistically significantly in the cells after UVB (10 and 50 mJ/cm²) exposure (Fig. 1A, Lanes 6, 8 vs. 5). Immunofluorescence detection of autophagosome formation in the HaCaT cells showed that HaCaT cells treated with UVB (10 and 25 mJ/cm²) and CQ form more intracellular aggregates of MAP1LC3A/B (Fig.

1B), which is correlated with the elevation of MAP1LC3A/B-II levels detected in the western blot (Fig. 1A). These results indicated that UVB induces both autophagosome formation and degradation.

UVB-induced autophagy response in HaCaT cells is cNOS-dependent.

To determine if cNOS plays a role in regulation of the dynamic autophagy response after UVB radiation, we analysed the effect of L-NAME (1 mM), a selective inhibitor of cNOS, on MAP1LC3A/B-II in HaCaT cells without or with UVB exposure. Our data shows that MAP1LC3A/B-II in HaCaT was not statistically significantly affected by L-NAME alone without or with UVB exposure (Fig. 2, Lanes 2 vs. 1, 3-5 vs. 2). However, in the presence of CQ, MAP1LC3A/B-II in L-NAME-treated cells was increased by approximately 29% without UVB exposure (Fig. 2, lanes 7 vs. 6); and reduced by approximately 39 or 28% in the cells with 25 or 50 mJ/cm² of UVB exposure, respectively (Fig. 2, Lanes 9 and 10 vs. 7). These results indicated that cNOS plays differential roles in regulation of background autophagy and dynamic autophagy responses to UVB irradiation.

UVB-induced cNOS-mediated dynamic autophagy responses are time-dependent.

To analyse the temporal autophagy response after UVB, we evaluated MAP1LC3A/B-II protein levels at 1 and 6 h after UVB. As it was observed in the 3 h experiment, the level of MAP1LC3A/B-II was not altered in HaCaT cells after UVB exposure alone (Fig. 3A). In the presence of CQ, at 1 h after UVB, MAP1LC3A/B-II was increased non-statistically significantly by approximately 20% and 25% in HaCaT cells after UVB at 10 and 25 mJ/cm² respectively; and increased statistically significantly by approximately 50% in cells after UVB at 50 mJ/cm² (Fig. 3A). Nonetheless, at 6 h after UVB, MAP1LC3A/B-II was decreased statistically significantly compared to the control after UVB 50 mJ/cm² (Fig. 3A). The extend of the effect of L-NAME on autophagy was also evaluated at 1 h and 6 h after UVB. In the presence of CQ, MAP1LC3A/B-II was increased by approximately 50% at 1 h (Fig. 3B), but non-statistically significantly changed at 6 h after treatment of L-NAME alone (Fig. 3B). Similar to the effect observed at 3 h (Fig. 2), L-NAME treatment led to a reduction of MAP1LC3A/B-II by approximately 28% and 47% at 1 h and 6 h after UVB (50 mJ/cm²), respectively (Fig. 3B). These results indicated that the cNOS-mediated

regulation of dynamic autophagy response post-UVB is time-dependent.

cNOS regulated SQSTM1/p62 expression post-UVB is autophagy-independent.

To determine if UVB-induced cNOS mediated autophagy response regulates the expression of sequestosome-1 (SQSTM1/p62), which is a known autophagy adaptor for substrate degradation (36), we analysed the effect of L-NAME (1 mM) on SQSTM1/p62 levels in HaCaT cells without or with UVB exposure. Our data shows that the SQSTM1/p62 level is decreased in HaCaT cells at 3 h after UVB exposure (Fig. 4A, Lines 2-4 vs. 1), and after treatment with L-NAME alone (Fig. 4A, line 5 vs. 1). The combined treatment of L-NAME and UVB further reduced SQSTM1/p62 expression in the cells with statistical significance (Fig. 4A, Lanes 6-8 vs. 5). In the presence of CQ, the SQSTM1/p62 level was not changed without UVB exposure (Fig. 4A, Lanes 9 vs. 1), and was decreased in the cells in a UVB dose-dependent manner (Fig. 4A, Lanes 10-12 vs. 9). The treatment of CQ statistically significantly alters the effect of L-NAME, decreasing further the levels of SQSTM1/p62 (Fig. 4A, Lane 13 vs. 5). CQ did not significantly alter the combination of UVB and L-NAME on SQSTM1/p62 levels (Fig. 4A, Lanes 14-16 vs. 6-8). The UVB dose-dependent reduction of SQSTM1/p62 after CQ treatment was confirmed by immunofluorescent staining of SQSTM1/p62 in the cells (Fig. 4B). Comparing with the autophagy data showed in Figs. 1-2, these results suggest that L-NAME alters SQSTM1/p62 expression in an autophagy-independent manner.

Nitric oxide and peroxynitrite are involved in the regulation of the autophagy response on HaCaT cells.

As cNOS regulates $\text{NO}^{\bullet}/\text{ONOO}^{-}$ balance in cells post-UVB, we determined that these molecules play a role in regulation of autophagosome synthesis in HaCaT cells after UVB exposure. A NO^{\bullet} donor S-Nitroso-N-acetyl-DL-penicillamine (SNAP) and an ONOO^{-} donor 3-Morpholino-sydnonimine (SIN-1) were used in the study. Our data showed that the level of MAP1LC3A/B-II was not altered by SNAP (Fig. 5A, Lanes 2-4 vs. 1), and was slightly increased without statistical significance by SIN-1 (Fig. 5B, Lanes 2-5 vs. 1). In the presence of CQ, the level of MAP1LC3A/B-II was increased by 24% in the cells after

SNAP (100 μM) treatment (Fig. 5A, Lane 8 vs. 5), and by > 40% in the cells after SIN-1 (5 and 30 μM) treatment (Fig. 5B, Lanes 8, 10 vs. 6). Higher doses of SIN-1 (500 to 1500 μM) were also tested but did not result in any significant autophagic response in the cells (data not shown). These results indicated that deregulation of either NO^{\bullet} or ONOO^{-} could have an effect on autophagosome synthesis.

The dynamic of autophagy response after UVB varies in different cell lines.

To determine the cell line-dependency of autophagy response, we analysed the effect of UVB on MAP1LC3A/B-II expression in the presence or absence of CQ and L-NAME in two primary keratinocytes cells lines; adult's human keratinocytes (HEKa) and neonatal's human keratinocytes (HEKn) (with passages ≤ 6). In addition, a non-keratinocyte cell line, the mouse embryonic fibroblast (MEF) cells; which has shown autophagy activation after UVB (21), was used to compare our results regarding the role of cNOS in autophagy regulation after UVB in keratinocytes. Our data showed that in HEKa cells at 1 h, but not at 3 h (data not shown) after UVB exposure in the presence of CQ, MAP1LC3A/B-II was increased statistically significant after 10, 25, and 50 mJ/cm^2 (Fig. 6A). As in HaCaT cells, MAP1LC3A/B-II levels increased by L-NAME alone, while L-NAME plus UVB mostly decreases them (Fig 6A). In the HEKn cells at 3 h post UVB, MAP1LC3A/B-II levels in the presence of CQ also increased significantly after UVB (25 mJ/cm^2). In the presence of L-NAME plus CQ, MAP1LC3A/B-II protein levels increased significantly by about 78%, but this increase was suppressed after UVB under cNOS inhibition (Fig. 6B). Finally, MEF cells evaluated at 3 h after UVB, effectively showed an increased level of MAP1LC3A/B-II by approximately 100% after UVB exposure alone (50 mJ/cm^2) (Fig. 6C); and the increase was not affected by L-NAME (Fig. 6C). In the presence of CQ, MAP1LC3A/B-II was increased 45% after UVB exposure alone (Fig. 6C). Similar to the results obtained in all the keratinocyte lines, the increase of MAP1LC3A/B-II was diminished in the presence of L-NAME post-UVB (Fig. 6C). These results demonstrated that the UVB-induced dynamic autophagy response is regulated by cNOS in all the evaluated cells lines with a potential shifting of time frame.

Discussion

Previous reports indicate that either UVB or NO[•] could induce or inhibit autophagy (21, 23). Our previous studies demonstrated that UVB induced the cNOS-mediated release of NO[•], which could quickly react with O₂^{•-} to form ONOO⁻, and led to NO[•]/ONOO⁻ imbalance in HaCaT cells (4). However, the role of NO[•] and ONOO⁻ in regulation of autophagy in UVB-exposed cells has not been well elucidated. In this study, we systematically analysed the effects of cNOS inhibitor as well as NO[•] and ONOO⁻ donors on UVB-induced autophagy response. Due to several contradictory reports on the mechanisms of UVB-induced autophagy, we first analysed the autophagic flux, including both autophagosome synthesis and degradation, in HaCaT cells post-UVB. Our data showed that MAP1LC3A/B-II levels were first increased (at 1 and 3 h post-UVB) and then decreased (at 6 h post-UVB) in HaCaT cells, only in the presence of CQ (Fig. 1 and Fig. 3A), suggesting UVB-induced autophagy response with similar effects on both synthesis and degradation of autophagosome. The analysis of autophagy in HEK293A and HEK293T corroborates that UVB increases the synthesis of autophagosomes (Fig. 6A and 6B). However, the time frame for this response was different between these three keratinocytes cells (Figs. 1, 3A, 6A, and 6B). Since autophagy is a dynamic process that depends of many regulators, some differences between cell lines are expected. In fact, we observed that, in HEK293A cells, the induction of autophagy happened at 1 h post-UVB (Fig. 6A), but not much changed at 3 h post-UVB (data not shown) as the other cell lines did (Figs. 1, 6B and 6C). Differences in functional properties have been described previously between neonatal and adult cells lines, as well as differences in gene expression profile and in the differentiation potential (37, 38). In addition, our data also indicated that the autophagy response, either synthesis or degradation of autophagosome, post-UVB is not linearly correlated to the doses of UVB (Figs. 1, 3, and 6), but mostly to a combination between the time of measurement and UVB dose. All of these results could be summarized to that UVB-induced autophagy response is a dynamic process with an up- or down-regulation of the synthesis and/or degradation of autophagosome in cell line- and UVB-dose dependent manners.

An analysis of the role of cNOS in the regulation of UVB-induced autophagy response showed that L-NAME did not have significant effects on the MAP1LC3A/B-II level in all cell lines without or with UVB exposure (Figs. 2, 3B, and 6), suggesting cNOS activity does not play a role in regulation of dynamic balance of autophagosome synthesis and degradation before and after UVB exposure. However, in the presence of CQ without UVB exposure, L-NAME either had no significant effect on MAP1LC3A/B-II in MEF cells (Fig. 6C) or increased MAP1LC3A/B-II in HaCaT, HEK293, and HEK293T cells at short incubation time (Fig. 2, Lane 7 vs. 6; Figs. 3B, 6A and 6B) indicating the background activity of cNOS has an inhibitory effect on both synthesis and the degradation of autophagosome in selective cell line(s). Interestingly, in the presence of CQ with UVB exposure, L-NAME reduced MAP1LC3A/B-II levels in all four tested cell lines (Figs. 2 vs. 1A; Figs. 3B vs. 3A, and 6), suggesting that UVB-induced activation of cNOS up-regulates both synthesis and degradation of autophagosome in cells. In addition, L-NAME treatment also led to a reduction of the UVB-induced MAP1LC3A/B-II by approximate 25% in samples 1 h after UVB 50 mJ/cm² (Fig. 3B vs. Fig. 3A) and in samples 3 h after UVB 25 mJ/cm² (Fig. 1A, Lane 7 vs. Fig. 2, Lane 9). The mechanisms of cNOS in up- and down-regulation of autophagy response could be due to a shift of cNOS-mediated imbalance of [NO•]/[ONOO⁻] post-UVB (4). Without UVB exposure, cNOS produces a background level of NO• in a range of picomole to nanomole (39) that helps to maintain a healthy [NO•]/[ONOO⁻] balance and to keep basal levels of autophagy (8, 40, 41). Then, the inhibition of cNOS without UVB exposure could alter the healthy [NO•]/[ONOO⁻] balance, inducing a stressed cellular condition that favours the synthesis of autophagosomes. After UVB exposure, cNOS mediates an increase of NO• and ONOO⁻, as well as an imbalance of [NO•]/[ONOO⁻] ratio due to the production of O₂^{•-} by cNOS uncoupling (4). A higher level of NO• or ONOO⁻ could be responsible for the increased autophagy response because previous reports (5, 6, 10) and our data show that either NO• donor SNAP or ONOO⁻ donor SIN-1 are able to induce autophagy in HaCaT cells (Figs. 5A and 5B). Our conclusion is supported by our previous reports indicating that a short period of pre-incubation of either a cNOS inhibitor or an antioxidant inhibits UVB-induced cell apoptosis (2, 4). Since autophagy is a mechanism for removing damaged cellular molecules and promoting cell survive in most cases, the only explanation for the

mechanism of action of L-NAME in inhibition of both apoptosis and autophagy post-UVB is that L-NAME is not a direct inhibitor of autophagy. Instead, it reduces UVB-induced stress, such as imbalance of NO^* / ONOO^- , which could lead to the activation of both autophagy and apoptosis.

In this study, we also analysed the expression of SQSTM1/p62, which has been described as one of the markers for autophagy (33). Our data showed that the levels of SQSTM1/p62 were decreased in the cells after UVB exposure (Fig. 4). However, the reduction of SQSTM1/p62 observed in HaCaT (Fig. 4) and HEKa cells (data not shown) was not correlated with the increase of MAP1LC3A/B-II in HaCaT cells after UVB exposure (Fig. 4 vs. 1A), nor with the levels of MAP1LC3A/B-II in HEKa cells (Fig. 6A). Because transcription of SQSTM1/p62 is not altered by UVB (data not shown), our results suggested that UVB-induced translational inhibition (24, 42, 43) might contribute to the downregulation of SQSTM1/p62 expression after UVB exposure in keratinocytes. In contrast to the observed in other tissues, regulation of SQSTM1/p62 protein levels independent of autophagy has been suggested previously in keratinocytes isolated from Atg7-deficient mice (44, 45).

A model for the role of cNOS in the regulation of autophagy in cells without or with UVB exposure is proposed (Fig. 7). Based on our results, without UVB exposition keratinocyte cells showed basal levels of autophagy, which are regulated by cNOS. However, after UVB exposition, the increased production of NO^* and ONOO^- is responsible of the induction of the autophagy flux in the four cell lines tested.

Funding:

This work was partially supported by NIH CA086928 and ES030425 (to S Wu), NSF1455554 IDBR: TYPE A (to H Chen and S Wu), and a graduate student scholarship from the Department of Chemistry and Biochemistry at Ohio University (to V. Bahamondes Lorca).

Conflicts of interest

There are no conflicts to declare.

Acknowledgements

We would like to thank Mary Kate McCulloch for editorial assistant in preparing this manuscript.

References

1. Chang HR, Tsao DA, Wang SR, Yu HS. Expression of nitric oxide synthases in keratinocytes after UVB irradiation. *Arch Dermatol Res.* 2003;295(7):293-6.
2. Liu W, Wu S. Differential roles of nitric oxide synthases in regulation of ultraviolet B light-induced apoptosis. *Nitric Oxide.* 2010;23(3):199-205.
3. Raad H, Serrano-Sanchez M, Harfouche G, Mahfouf W, Bortolotto D, Bergeron V, et al. NADPH Oxidase-1 Plays a Key Role in Keratinocyte Responses to UV Radiation and UVB-Induced Skin Carcinogenesis. *J Invest Dermatol.* 2017;137(6):1311-21.
4. Wu S, Wang L, Jacoby AM, Jasinski K, Kubant R, Malinski T. Ultraviolet B light-induced nitric oxide/peroxynitrite imbalance in keratinocytes--implications for apoptosis and necrosis. *Photochem Photobiol.* 2010;86(2):389-96.
5. Datta S, Chakraborty S, Panja C, Ghosh S. Reactive nitrogen species control apoptosis and autophagy in K562 cells: implication of TAp73alpha induction in controlling autophagy. *Free Radic Res.* 2018;52(4):491-506.
6. He H, Feng Y-S, Zang L-H, Liu W-W, Ding L-Q, Chen L-X, et al. Nitric oxide induces apoptosis and autophagy; autophagy down-regulates NO synthesis in physalin A-treated A375-S2 human melanoma cells. *Food and Chemical Toxicology.* 2014;71:128-35.
7. Lee J, Giordano S, Zhang J. Autophagy, mitochondria and oxidative stress: cross-talk and redox signalling. *Biochem J.* 2012;441(2):523-40.
8. Sarkar S, Korolchuk VI, Renna M, Imarisio S, Fleming A, Williams A, et al. Complex inhibitory effects of nitric oxide on autophagy. *Mol Cell.* 2011;43(1):19-32.
9. Scherz-Shouval R, Shvets E, Fass E, Shorer H, Gil L, Elazar Z. Reactive oxygen species are essential for autophagy and specifically regulate the activity of Atg4. *EMBO J.* 2007;26(7):1749-60.
10. Tripathi DN, Chowdhury R, Trudel LJ, Tee AR, Slack RS, Walker CL, et al. Reactive nitrogen species regulate autophagy through ATM-AMPK-TSC2-mediated suppression of mTORC1. *Proc Natl Acad Sci U S A.* 2013;110(32):E2950-7.
11. Kim KH, Lee MS. Autophagy--a key player in cellular and body metabolism. *Nat Rev Endocrinol.* 2014;10(6):322-37.
12. Aymard E, Barruche V, Naves T, Bordes S, Closs B, Verdier M, et al. Autophagy in human keratinocytes: an early step of the differentiation? *Exp Dermatol.* 2011;20(3):263-8.
13. Haruna K, Suga Y, Muramatsu S, Taneda K, Mizuno Y, Ikeda S, et al. Differentiation-specific expression and localization of an autophagosomal marker protein (LC3) in human epidermal keratinocytes. *J Dermatol Sci.* 2008;52(3):213-5.
14. Li L, Chen X, Gu H. The signaling involved in autophagy machinery in keratinocytes and therapeutic approaches for skin diseases. *Oncotarget.* 2016;7(31):50682-97.
15. Murase D, Hachiya A, Takano K, Hicks R, Visscher MO, Kitahara T, et al. Autophagy has a significant role in determining skin color by regulating melanosome degradation in keratinocytes. *J Invest Dermatol.* 2013;133(10):2416-24.
16. Griffin LM, Cicchini L, Pyeon D. Human papillomavirus infection is inhibited by host autophagy in primary human keratinocytes. *Virology.* 2013;437(1):12-9.
17. Lee HM, Shin DM, Yuk JM, Shi G, Choi DK, Lee SH, et al. Autophagy negatively regulates keratinocyte inflammatory responses via scaffolding protein p62/SQSTM1. *J Immunol.* 2011;186(2):1248-58.

18. Deruy E, Nassour J, Martin N, Vercamer C, Malaquin N, Bertout J, et al. Level of macroautophagy drives senescent keratinocytes into cell death or neoplastic evasion. *Cell Death Dis.* 2014;5:e1577.
19. Gosselin K, Deruy E, Martien S, Vercamer C, Bouali F, Dujardin T, et al. Senescent keratinocytes die by autophagic programmed cell death. *Am J Pathol.* 2009;174(2):423-35.
20. Song X, Narzt MS, Nagelreiter IM, Hohensinner P, Terlecki-Zaniewicz L, Tschachler E, et al. Autophagy deficient keratinocytes display increased DNA damage, senescence and aberrant lipid composition after oxidative stress in vitro and in vivo. *Redox Biol.* 2017;11:219-30.
21. Qiang L, Wu C, Ming M, Viollet B, He YY. Autophagy controls p38 activation to promote cell survival under genotoxic stress. *J Biol Chem.* 2013;288(3):1603-11.
22. Sample A, He YY. Autophagy in UV Damage Response. *Photochem Photobiol.* 2017;93(4):943-55.
23. Chen X, Li L, Xu S, Bu W, Chen K, Li M, et al. Ultraviolet B radiation down-regulates ULK1 and ATG7 expression and impairs the autophagy response in human keratinocytes. *J Photochem Photobiol B.* 2018;178:152-64.
24. Lu W, Laszlo CF, Miao Z, Chen H, Wu S. The role of nitric-oxide synthase in the regulation of UVB light-induced phosphorylation of the alpha subunit of eukaryotic initiation factor 2. *J Biol Chem.* 2009;284(36):24281-8.
25. Tong L, Wu S. The role of constitutive nitric-oxide synthase in ultraviolet B light-induced nuclear factor kappaB activity. *J Biol Chem.* 2014;289(38):26658-68.
26. Comb WC, Cogswell P, Sitcheran R, Baldwin AS. IKK-dependent, NF-kappaB-independent control of autophagic gene expression. *Oncogene.* 2011;30(14):1727-32.
27. Criollo A, Senovilla L, Authier H, Maiuri MC, Morselli E, Vitale I, et al. The IKK complex contributes to the induction of autophagy. *EMBO J.* 2010;29(3):619-31.
28. Kim KW, Moretti L, Mitchell LR, Jung DK, Lu B. Endoplasmic reticulum stress mediates radiation-induced autophagy by perk-eIF2alpha in caspase-3/7-deficient cells. *Oncogene.* 2010;29(22):3241-51.
29. Rouschop KM, van den Beucken T, Dubois L, Niessen H, Bussink J, Savelkoul K, et al. The unfolded protein response protects human tumor cells during hypoxia through regulation of the autophagy genes MAP1LC3B and ATG5. *J Clin Invest.* 2010;120(1):127-41.
30. Rzymiski T, Milani M, Pike L, Buffa F, Mellor HR, Winchester L, et al. Regulation of autophagy by ATF4 in response to severe hypoxia. *Oncogene.* 2010;29(31):4424-35.
31. Shi K, An J, Shan L, Jiang Q, Li F, Ci Y, et al. Survivin-2B promotes autophagy by accumulating IKK alpha in the nucleus of selenite-treated NB4 cells. *Cell Death Dis.* 2014;5:e1071.
32. Trocoli A, Djavaheri-Mergny M. The complex interplay between autophagy and NF-kB signaling pathways in cancer cells. *Am J Cancer Res.* 2011;1(5):629-49.
33. Klionsky DJ, Abdelmohsen K, Abe A, Abedin MJ, Abeliovich H, Acevedo Arozena A, et al. Guidelines for the use and interpretation of assays for monitoring autophagy (3rd edition). *Autophagy.* 2016;12(1):1-222.
34. Mizushima N, Yoshimori T, Levine B. Methods in mammalian autophagy research. *Cell.* 2010;140(3):313-26.

35. Mauthe M, Orhon I, Rocchi C, Zhou X, Luhr M, Hijlkema KJ, et al. Chloroquine inhibits autophagic flux by decreasing autophagosome-lysosome fusion. *Autophagy*. 2018;14(8):1435-55.
36. Sanchez-Martin P, Saito T, Komatsu M. p62/SQSTM1: 'Jack of all trades' in health and cancer. *FEBS J*. 2019;286(1):8-23.
37. Mateu R, Zivicova V, Krejci ED, Grim M, Strnad H, Vlcek C, et al. Functional differences between neonatal and adult fibroblasts and keratinocytes: Donor age affects epithelial-mesenchymal crosstalk in vitro. *Int J Mol Med*. 2016;38(4):1063-74.
38. Krejci E, Kodet O, Szabo P, Borsky J, Smetana K, Jr., Grim M, et al. In vitro differences of neonatal and later postnatal keratinocytes and dermal fibroblasts. *Physiol Res*. 2015;64(4):561-9.
39. Hall CN, Garthwaite J. What is the real physiological NO concentration in vivo? *Nitric Oxide*. 2009;21(2):92-103.
40. Thomas DD, Ridnour LA, Isenberg JS, Flores-Santana W, Switzer CH, Donzelli S, et al. The chemical biology of nitric oxide: implications in cellular signaling. *Free Radic Biol Med*. 2008;45(1):18-31.
41. Zhu L, Li L, Zhang Q, Yang X, Zou Z, Hao B, et al. NOS1 S-nitrosylates PTEN and inhibits autophagy in nasopharyngeal carcinoma cells. *Cell Death Discov*. 2017;3:17011.
42. Collier AE, Wek RC, Spandau DF. Translational Repression Protects Human Keratinocytes from UVB-Induced Apoptosis through a Discordant eIF2 Kinase Stress Response. *J Invest Dermatol*. 2015;135(10):2502-11.
43. Wu S, Hu Y, Wang JL, Chatterjee M, Shi Y, Kaufman RJ. Ultraviolet light inhibits translation through activation of the unfolded protein response kinase PERK in the lumen of the endoplasmic reticulum. *J Biol Chem*. 2002;277(20):18077-83.
44. Rossiter H, Konig U, Barresi C, Buchberger M, Ghannadan M, Zhang CF, et al. Epidermal keratinocytes form a functional skin barrier in the absence of Atg7 dependent autophagy. *J Dermatol Sci*. 2013;71(1):67-75.
45. Sukseree S, Bergmann S, Pajdzik K, Tschachler E, Eckhart L. Suppression of autophagy perturbs turnover of sequestosome-1/p62 in Merkel cells but not in keratinocytes. *J Dermatol Sci*. 2018;90(2):209-11.

Figure legends

Figure 1. Autophagy response of HaCaT cells after UVB irradiation. HaCaT cells were exposed to 10, 25 and 50 mJ/cm² UVB radiation with and without chloroquine (CQ, 50 μM) and collected 3 h post-UVB radiation. The expression levels of MAP1LC3A/B and its location were measured respectively by Western blot and immunofluorescent analysis. (A) Western blot and statistical analysis of MAP1LC3A/B-II (LC3-II) in cells treated without or with CQ and UVB at different doses. (B) immunofluorescence staining of MAP1LC3A/B (green) on HaCaT cells treated with CQ and UVB radiation. Bar 20 μm, nuclei (blue), arrows show MAP1LC3A/B aggregates. * = statistical analysis against 0 mJ/cm² plus CQ. p <0.05 was considered significant.

Figure 2. cNOS is involved in the autophagy response after UVB. HaCaT cells were exposed to 10, 25, and 50 mJ/cm² UVB radiation with and without L-NAME (1 mM) and CQ (50 μM) as indicated and collected 3 h post-UVB radiation. Western blot showing the effect of L-NAME on the MAP1LC3A/B-II (LC3-II) protein levels on HaCaT cells post UVB in the presence or absence of CQ. Statistical analysis on HaCaT cells showing the effect of L-NAME and UVB on the expression of MAP1LC3A/B-II (LC3-II) in the presence or absence of CQ. ° = statistical analysis against 0 mJ/cm² CQ, + = statistical analysis against 0 mJ/cm² L-NAME plus CQ. p <0.05 was considered significant.

Figure 3. Autophagy response of HaCaT cells after UVB irradiation at 1 h and 6 h after UVB exposition with and without L-NAME. HaCaT cells were exposed to 10, 25 and 50 mJ/cm² UVB radiation with and without chloroquine (CQ, 50 μM) and/or L-NAME (1 mM). The expression levels of MAP1LC3A/B-II (LC3-II) were determined by Western blot analysis. (A) Statistical analysis of MAP1LC3A/B-II (LC3-II) in cells treated without or with CQ and UVB at different doses and incubated after irradiation during 1h (white bar) and 6 h (dark grey bar). (B) Statistical analysis of MAP1LC3A/B-II (LC3-II) in cells treated without or with CQ, L-NAME, and UVB at different doses; and incubated after irradiation during 1h (white bars) and 6 h (dark grey bars). * = statistical analysis against 0 mJ/cm², ° = statistical analysis against 0 mJ/cm² plus CQ, + = statistical analysis against 0 mJ/cm² L-NAME plus CQ. p <0.05 was considered significant.

Figure 4. Evaluation of SQSTM1/p62 expression in HaCaT cells after UVB. HaCaT cells were treated with UVB (10, 25, and 50 mJ/cm²), CQ (50 μM) and L-NAME (1 mM) as indicated and collected 3 h post UVB. (A) Western blot and statistical analysis of SQSTM1/p62 on HaCaT cells irradiated with UVB and without or treated continuously with L-NAME and/or CQ. * = statistical analysis against 0 mJ/cm² control, # = statistical analysis against 0 mJ/cm² L-NAME, ° = statistical analysis against 0 mJ/cm² plus CQ, • = statistical analysis against their pairs without L-NAME. p <0.05 was considered significant. (B) immunofluorescence staining of SQSTM1/p62 (green) on HaCaT cells 3 h post UVB radiation. Bar 20 μm, nuclei (blue). Arrows indicate SQSTM1/p62 forming aggregates.

Figure 5. Role of nitric oxide and peroxynitrite in the autophagy response on HaCaT cells. HaCaT cells were treated with NO[•] and ONOO⁻ donors as indicated for 3 h. (A) Western blot and statistical analysis of MAP1LC3A/B-II (LC3-II) protein levels on HaCaT cells treated with the NO[•] donor SNAP at different concentrations as indicated, and in the presence or absence of CQ. (B) Western blot and statistical analysis of MAP1LC3A/B-II (LC3-II) protein levels on HaCaT cells treated with the ONOO⁻ donor SIN-1 at different concentrations as indicated, in the presence or absence of CQ. * = statistical analysis against 0 mJ/cm² plus CQ. p <0.05 was considered significant.

Figure 6. Evaluation of the autophagy response in adults and neonatal primary keratinocyte cell line (HEKa and HEKn respectively) and in a mouse embryonic fibroblast cell line (MEF). (A) Statistical analysis of MAP1LC3A/B-II (LC3-II) protein levels on HEKa cells exposed to 10, 25, and 50 mJ/cm² UVB radiation with and without L-NAME (1 mM) in the presence or absence of CQ (50 μM) as indicated and collected 1 h post-UVB radiation. (B) Statistical analysis of MAP1LC3A/B-II (LC3-II) protein levels on HEKn cells exposed to 10, 25, and 50 mJ/cm² UVB radiation with and without L-NAME (1 mM) in the presence or absence of CQ (50 μM) as indicated and collected 3 h post-UVB radiation. (C) Statistical analysis of MAP1LC3A/B-II (LC3-II) protein levels on MEF cells treated with or without UVB (50 mJ/cm²), L-NAME (1 mM), and CQ (50 μM) as indicated and collected 3 h post-UVB radiation. * = statistical analysis against 0 mJ/cm² control, # = statistical analysis against 0 mJ/cm² plus L-NAME, ° = statistical analysis against 0

mJ/cm² plus CQ, + = statistical analysis against 0 mJ/cm² L-NAME plus CQ, • = statistical analysis against their pairs without L-NAME. p <0.05 was considered significant.

Figure 7. Model for the role of cNOS in regulation of autophagy in cells without or with UVB exposure. Without UVB exposition, cells showed basal levels of autophagy, which are regulated by cNOS in a cell line specific way. However, after UVB exposition, the increased production of NO• and ONOO⁻ is responsible of the induction of the autophagy flux in the three cell lines tested.

Fig. 1

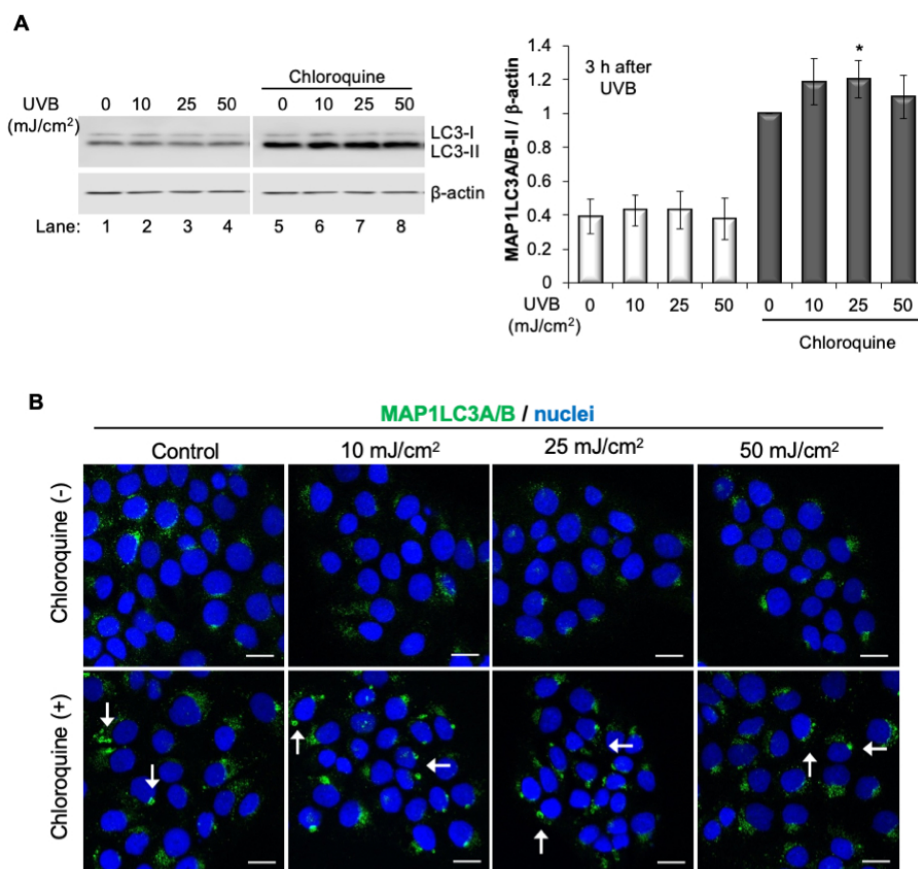
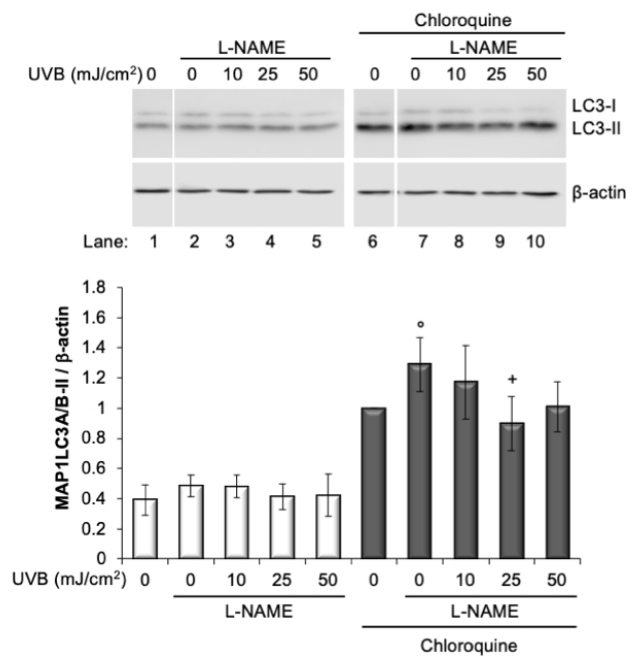


Fig1

76x98mm (300 x 300 DPI)

Fig. 2



Fgi2

76x98mm (300 x 300 DPI)

Fig. 3

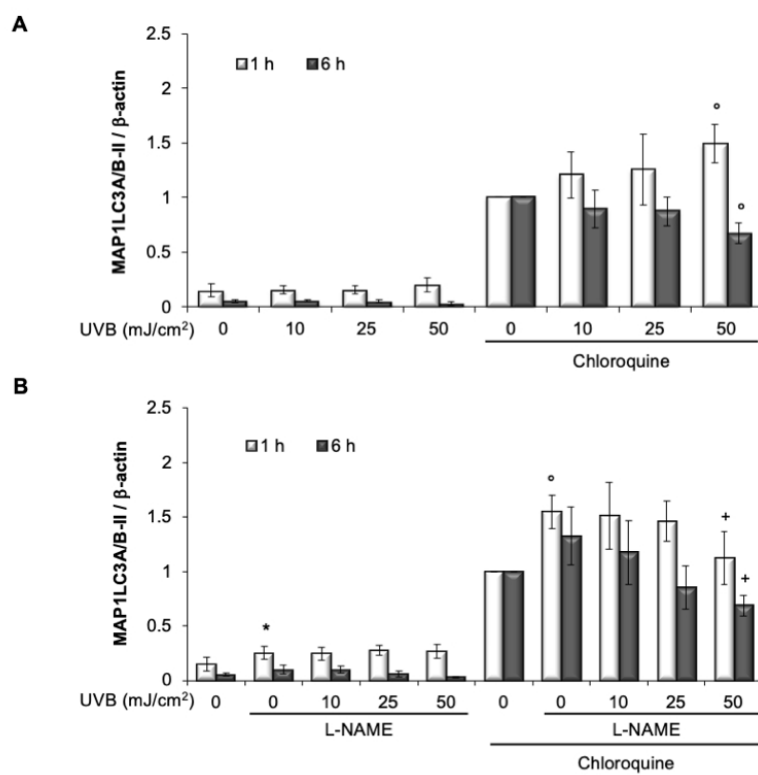


Fig3

76x98mm (300 x 300 DPI)

Fig. 4

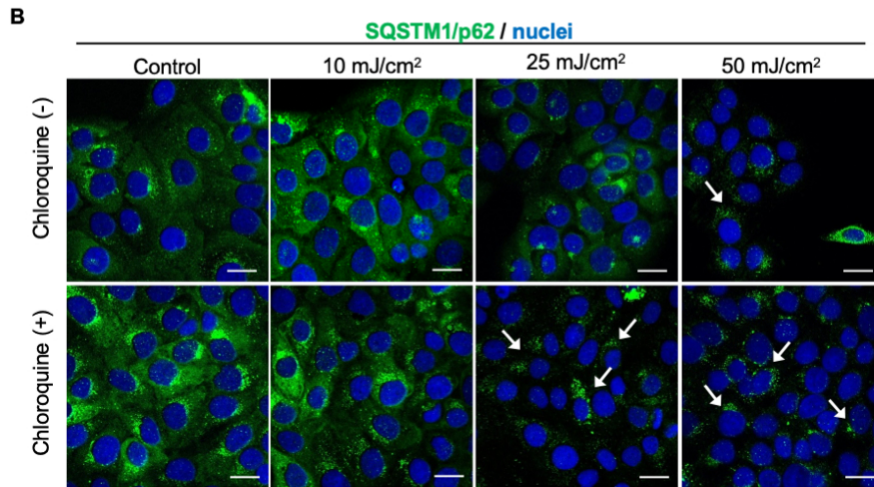
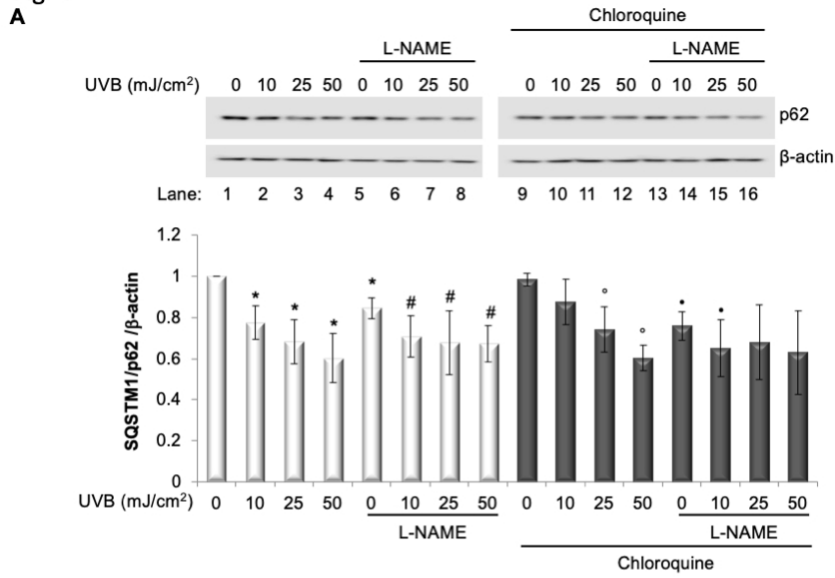


Fig4

78x101mm (300 x 300 DPI)

Fig. 5

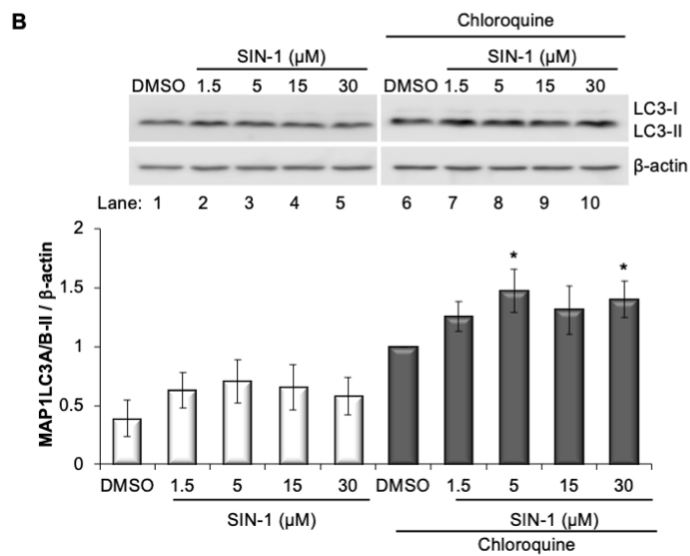
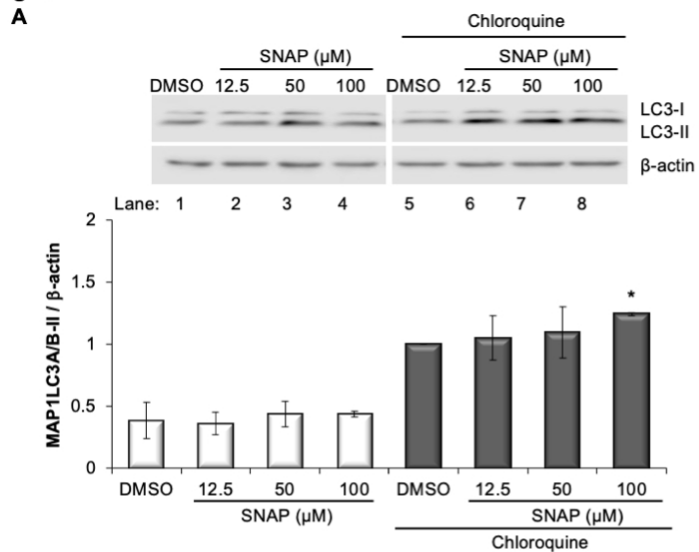


Fig5

78x101mm (300 x 300 DPI)

Fig. 6

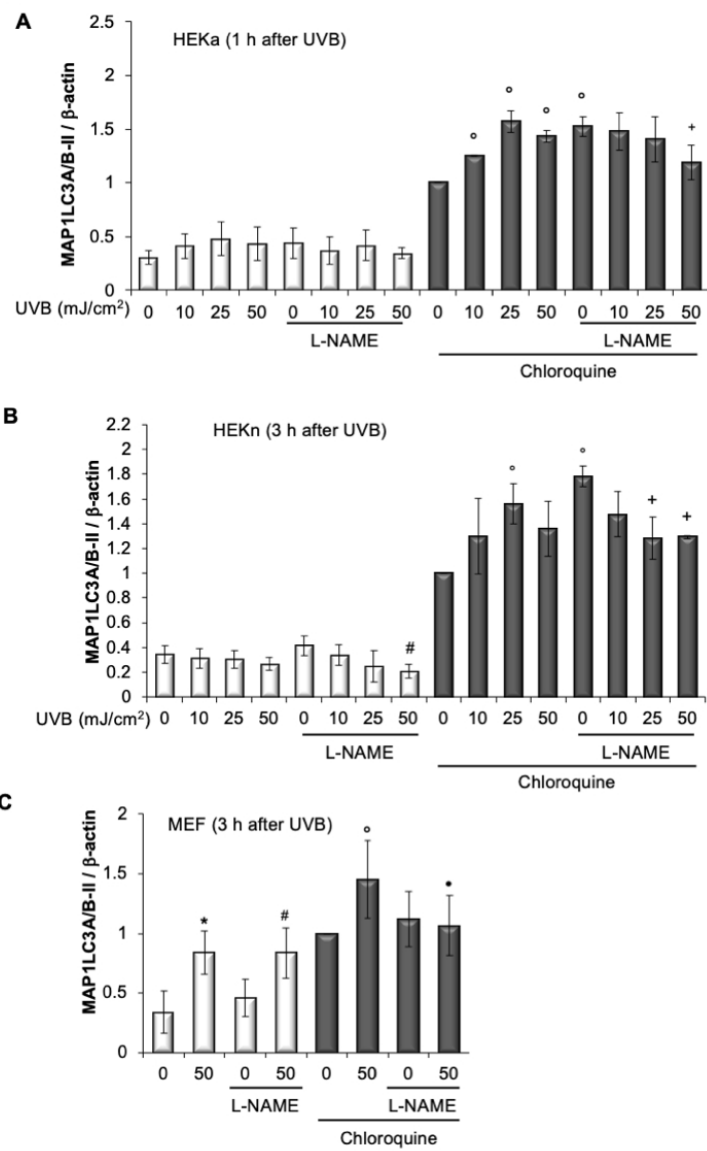


Fig6

76x98mm (300 x 300 DPI)

Fig. 7

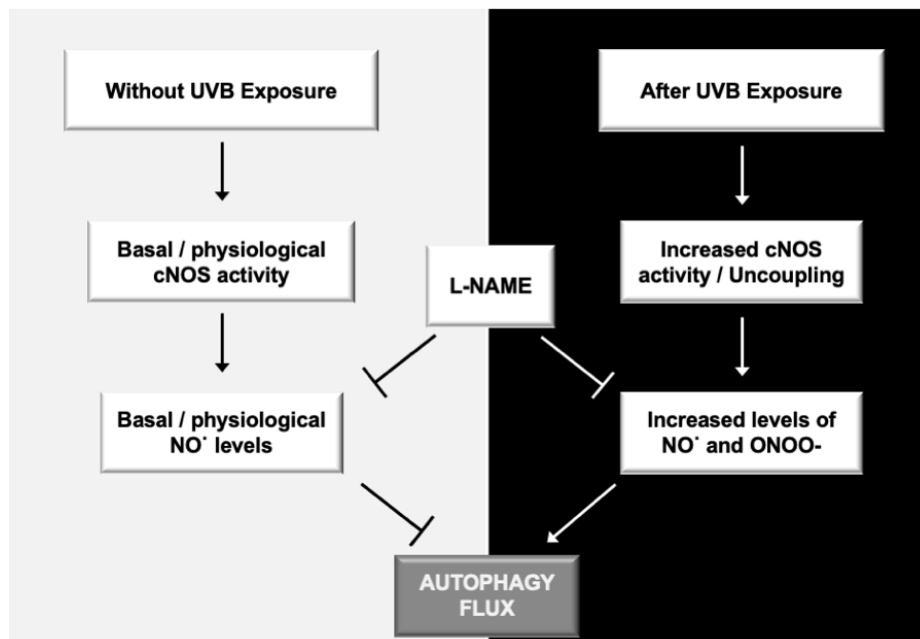


Fig7

76x98mm (300 x 300 DPI)